Use of phase change materials (PCMs) to mitigate early age thermal cracking in concrete
Theoretical considerations

Savija, Branko; Schlangen, Erik

DOI
10.1016/j.conbuildmat.2016.09.046

Publication date
2016

Document Version
Accepted author manuscript

Published in
Construction and Building Materials

Use of phase change materials (PCMs) to mitigate early age thermal cracking in concrete: theoretical considerations

Branko Šavija[1*] and Erik Schlangen[1]

1- Microlab, Faculty of Civil Engineering and Geosciences, Delft University of Technology
Stevinweg 1, 2628 CN Delft, the Netherlands
e-mail: b.savija@tudelft.nl; erik.schlangen@tudelft.nl

*- corresponding author, Tel: +31(0)15 27 88986, Fax: +31(0)15 27 86383

Article to be submitted to *CONSTRUCTION AND BUILDING MATERIALS*

Abstract

Phase change materials (PCMs) have found their use in concrete technology for increasing energy efficiency of building envelopes. In recent years, however, new potential applications for PCMs in concrete have been suggested, for example for reducing freeze-thaw damage and melting of ice forming on top of concrete pavements. A recent application of PCMs in concrete technology is their use for mitigating early-age cracking in hydrating concrete. The focus on this paper is therefore on theoretical considerations related to this particular application of phase change materials. In particular, the focus is on simulating microencapsulated PCMs, which show very promising experimental results. Numerical models are developed for 2 scales: the meso-scale, in which the PCM microcapsules are simulated as discrete inclusions in the cementitious matrix; and the macro-scale, where the effect of PCM microcapsule addition is considered in a smeared way. On the meso-scale, the effect of PCM volume percentage, their phase change temperature, and latent heat of fusion on simulated adiabatic heat evolution are assessed. On the macro-scale, influence of these parameters on the temperature evolution in semi-adiabatic (field) conditions and tensile stress development are simulated. The outcomes of this study provide valuable insights related to the influence of PCM microcapsule parameters on the behaviour of cementitious materials, enabling tailoring composites for different environmental conditions.

Keywords: Phase Change Materials (PCMs); Heat evolution; Thermal cracking; Numerical modelling; Lattice modelling

1. Introduction

During construction, temperature in concrete will increase due to exothermic hydration reactions of cement. If unrestrained, the concrete in a structural element expands and contracts during the early-age heating and the subsequent cooling process without stresses being induced [1]. In practice, however, the concrete is nearly always restrained to some degree, either externally by adjoining structures or internally by different temperatures in the components of the structure itself [1]. This is an issue especially in massive hardening concrete structures which are most prone to thermal cracking at early age due to the hydration heat of cement [2-4]. As the surface of the structure will lose heat to the atmosphere, a thermal gradient will appear between the cold outside and the warm core of the structure or element. Differences in free thermal dilation between various parts of the structure will give rise to tensile stresses at the surface [5]. If these stresses exceed the tensile strength of concrete, cracking will occur. This is a common problem in engineering practice, and may be aggravated by unfavourable environmental conditions during concrete casting and curing [6]. Definition of mass concrete is somewhat ambiguous, with ACI 116R defining is "any volume of concrete with dimensions large enough to require that measures be taken to cope with generation of heat from hydration of the cement and attendant volume change, to minimize cracking"[7]. Different agencies give more specific guidelines, such as defining any concrete element having a least dimension greater than 0.9 m as mass concrete [8]. Currently, mass concrete is no longer considered only for dam construction; it is also used for foundation and members of structures for many classes as multistorey and nuclear reactor buildings [9, 10].

Cracks occurring at early age do not necessarily pose a threat to structural safety. However, these cracks can increase the susceptibility of the structure to environmental attacks, such as chloride ingress [11, 12]. This can result in a significant reduction of the service life [13]. The occurrence of thermal cracks depends, in general, on 3 groups of factors [14]: (1) material factors, which are related to mix proportions, cement type, and admixtures used; (2) structural factors, related mainly to internal and external restraints on the structure/element; and (3) execution factors, related to placing temperature, curing, insulation, etc. Therefore, different measures can be used to tackle this issue, ranging from simple changes in mix design (e.g. using lower cement content [4] or blended cements [15]), structural modifications (e.g. expansion joints, additional reinforcement, prestressing [4, 14]), or execution parameters (cooling pipes or formwork) [16].

Another possibility for mitigating thermal cracking in hardening concrete has been recently proposed – the use of phase change materials (PCMs) as additives [17-20]. A phase change material has high heat of fusion which can, by melting and solidifying at a certain temperature, store and dissipate large amounts of energy in the form of heat [21]. In recent years, many studies have been devoted to the use of PCMs in cementitious materials to increase the energy efficiency of buildings [22-25]. Different ways of incorporating PCMs into concrete have been proposed: (1) impregnation in lightweight aggregates [17, 26, 27]; (2) microencapsulation [19, 24, 28, 29]; and (3) embedding in tubes [26, 30]. In this work, microencapsulated PCMs are considered.

Numerical simulation tools have also been proposed in the literature to assess the thermal performance and the efficiency of PCM modified concrete [31, 32]. The use of modelling tools can help in tailoring efficient PCM based composites. This study aims to evaluate the effects of adding microencapsulated PMCs in cement based systems on their thermal and structural performance. First, a meso-scale numerical tool for simulating temperature evolution in a composite system containing microencapsulated PCM is presented. This part focuses on material parameters related to PCM addition, such as the addition percentage, heat of fusion, and temperature of phase change. The next part deals with modelling of a full-scale hardening concrete structure using a commercial FE package, where the interaction of the structure with the environment is considered. The main focus of the second part is to assess the effect of PCM addition on stress evolution in the hardening structure. The influence of different parameters on temperature and stress development is discussed. This study will serve as a basis for design and development of PCM modified cement based materials and structures for mitigating thermal cracking in various environmental conditions.

2. Methods

2.1. Meso-scale modelling approach

Lattice models have long been used to simulate fracture processes in concrete [33-35] and other quasi-brittle materials [36, 37]. Unlike the continuum mechanics approaches, in this type of models the continuum is discretized as a set of two-node (truss or beam) elements which can transfer forces. Fracture is simulated by damaging these discrete elements. These models can be successfully used on multiple scales, from the micro-scale (i.e. cement paste scale [38]), to the meso-scale (i.e. mortar scale [35, 39]) and the macro-scale (i.e. concrete element and structure scale [40]). Different scales can be simulated in a straight-forward fashion by implementing the material structure appropriate for each scale.

Recently, the concept of lattice (or rather discrete) modelling has been extended to simulating transport processes in concrete, such as moisture [41, 42] transport, chloride transport [43-45], and electrical current flow [46]. In the transport model, the material domain is discretized as a set of one-dimensional “pipe” elements through which the transport takes place. This type of model is used herein.

For spatial discretization in three dimensions, the starting point is a prismatic domain. This domain is first divided into a number of cubic cells. Then, a sub-cell is defined in the centre of each cell. A node is randomly placed within each sub-cell using a pseudo-random number generator (Figure 1). Then, a Voronoi tessellation of the domain, with respect to the generated set of nodes, is performed. Nodes with adjacent Voronoi cells are connected by lattice elements (Figure 1) [40].

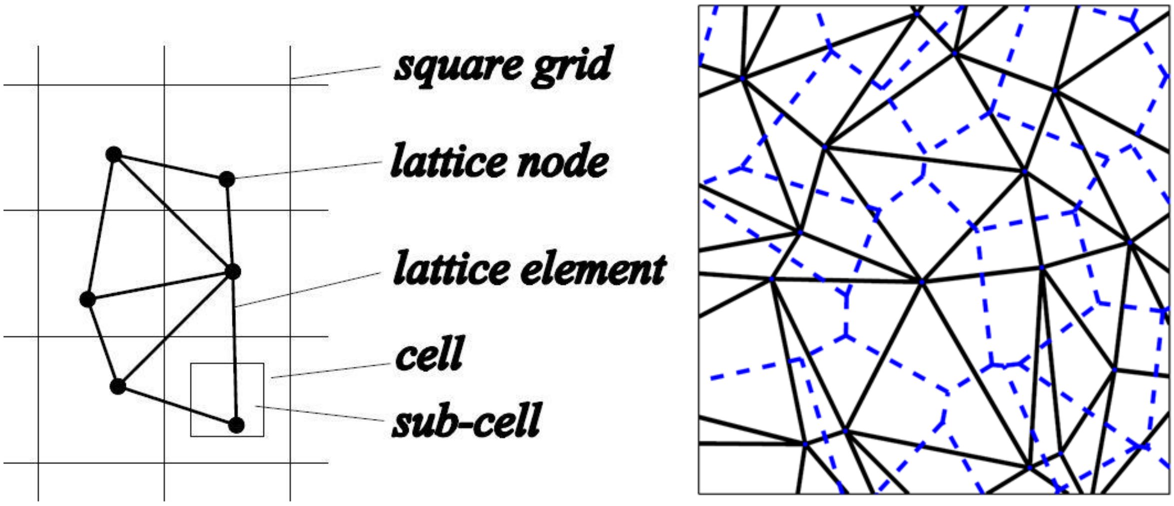

Figure 1. Left: Node placement procedure in two-dimensions. Right: Meshing procedure in two-dimensions. Solid, lattice; dashed, Voronoi cells.

Heterogeneous material behaviour can be considered by employing the particle overlay procedure (Figure 2). This way, properties can be assigned to different material phases. As an input, either a computer generated material structure, or a material structure obtained by scanning (2D) or CT-scanning (3D), can be used. Each node in the mesh is assigned with a pixel/voxel value (2D and 3D, respectively) from the used material structure. Properties assigned to each element depend on the pixel/voxel value at its end nodes (Figure 2).

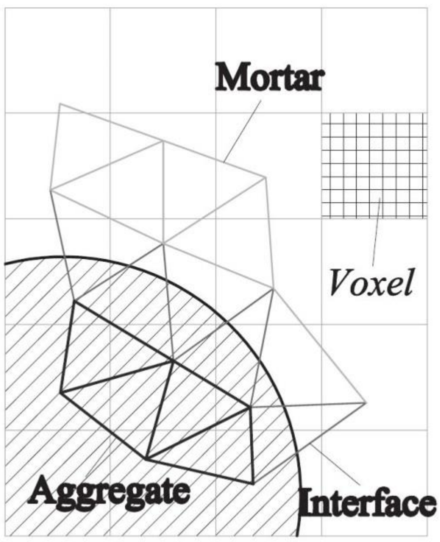

Figure 2. Particle overlay procedure in two dimensions

2.1.1. Heat transport model

To simulate the heat transport on this scale, the transient heat conduction equation for a stationary medium is used [47]:

$$\rho c_p \frac{\partial T}{\partial t} = \frac{\partial}{\partial x}\left(k \frac{\partial T}{\partial x} \right) + \dot{Q} \tag{1}$$

Here, ρ is the density (kg/m^3), c_p the specific heat capacity (J/kg·K), k the thermal conductivity (W/mK), T the temperature (K), t time (s), and x the spatial coordinate (m). The rate of heat production due to hydration is implemented through the source term $\dot{Q}$ (J/m^{3}s).

Equation (1) can be discretized in space using the standard Galerkin procedure [43, 47]. The following set of equation arises (in matrix form):

$$C \frac{\partial T}{\partial t} + KT = f \tag{2}$$

In equation (2), C is the element capacitance matrix, K the element conductivity matrix, and f the forcing vector. Vector of unknowns, T, is the vector of temperatures in the nodes of a lattice element. Elemental matrices in equation (2) have the following form:

$$C = \frac{Al\rho c_p}{6\omega} \begin{bmatrix} 2 & 1 \\ 1 & 2 \end{bmatrix} \tag{3}$$

$$K = \frac{kA}{l} \begin{bmatrix} 1 & -1 \\ -1 & 1 \end{bmatrix} \tag{4}$$

Here, l is the element length, A the element cross-sectional area. In the lattice approach, cross-sectional areas of individual lattice elements are assigned using the so-called Voronoi scaling method [40, 41] – cross sectional area of an element is equal to the area of a facet of a Voronoi cell which is common to its end nodes. Note that element capacitance and conductivity matrices are equivalent to those of regular 1D linear finite elements [47], except the non-dimensional correction parameter ω in the capacitance matrix (equation (3)). This parameter is used to convert the volume of a Voronoi cell to the volume of lattice elements, due to overlap of volume of adjacent lattice elements (Figure 3). It can be calculated as [48]:

$$\omega = \frac{\sum_{k=1}^{m} A_k \cdot l_k}{V} \tag{5}$$

where m is the total number of elements in the mesh, A_k and l_k cross sectional area and length of each lattice element, k element number, and V the volume of the specimen. It was shown that ω can be set as 2 for the two-dimensional and 3 for the three-dimensional case, respectively, without loss of accuracy [41].

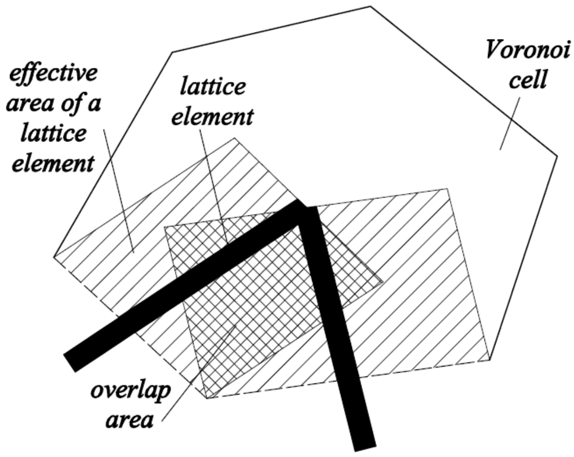

Figure 3. Definition of overlap area for determination of parameter ω (adapted from [48]).

The forcing vector, at this scale, considers only the internal development of hydration heat. Heat of hydration calculations are performed for each node using the volume of the corresponding Voronoi cell [6]. Therefore, forcing vector due to heat of hydration for each node is:

$$f_i = \dot{Q} V_i \tag{6}$$

where i is the node number, and V_i the volume of the corresponding Voronoi cell. System matrices are assembled using the standard finite element procedure [47].

The total heat absorbed by PCM microcapsules comprises a sensible heat contribution (proportional to the mass and the specific heat capacity of the material) and the latent heat contribution (proportional to the mass and the enthalpy of phase change) [19]. Most materials can absorb sensible heat: it is the latent heat contribution that provides the PCMs with their energy storage capacity. The latent heat stored during phase change in the PCM microcapsules is taken into account in the model by using the heat capacity method [23]. Contribution from the latent heat due to the phase change process is considered by using a piecewise temperature dependent function for the specific heat capacity of the PCM microcapsules [32, 49]:

$$c_p(T) = \begin{cases} c_{p,s} & \text{for } T < T_{pc} - \Delta T_{pc}/2 \\ c_{p,s} + \dfrac{h_f}{\Delta T_{pc}} & \text{for } T_{pc} - \Delta T_{pc}/2 \le T \le T_{pc} + \Delta T_{pc}/2 \\ c_{p,l} & \text{for } T > T_{pc} + \Delta T_{pc}/2 \end{cases} \qquad (7)$$

where $c_{p,s}$ and $c_{p,l}$ are the specific heat capacities of the solid and the liquid phase (it is assumed in all analyses that $c_{p,s}=c_{p,l}$), T_{pc} the phase change temperature, ΔT_{pc} the temperature window, and h_f the latent heat of fusion of the phase change material.

System of equations (2) is discretized in time using the Crank-Nicholson procedure [47]:

$$(C^{n-1} + 0.5\Delta t K)T^n = (C^{n-1} - 0.5\Delta t K)T^{n-1} + \Delta t \cdot f \qquad (8)$$

This equation is then solved for each discrete time step (Δt) and the temperature distribution is obtained. Since the specific heat capacity (c_p) and, therefore, matrix C is dependent on temperature T (for phase change microcapsules, see equation (7)), the iterative procedure is avoided by calculating temperature in each step (n) based on values of specific heat capacities from the previous step (n-1). Although this implies a certain amount of error, it significantly shortens the simulation time and the error is small for small time step Δt.

On the meso-scale, the material is considered to comprise a cementitious matrix and discrete microcapsules containing phase-change materials.

2.1.2. Model validation

For the validation of the discrete modelling approach, a homogeneous cement paste specimen was simulated. Material properties of the cement paste used in this simulation were given by Thiele et al. [32] (see Table 1).

Table 1. Material properties used in meso-scale simulations [32]. (Note that the PCM used in [32] was an organic paraffin encapsulated by a melamine-formaldehyde shell)

Material	ρ (kg/m^3)	c (J/kg K)	k (W/mK)
Cement paste	1965	1530	1
PCM	900	1900	0.42

For the development of heat of hydration, experimental results of De Schutter and Taerwe [50] are used[1]. They performed isothermal hydration tests for Portland Cement CEM I 52.5. One of their measurements (at 35 °C) is used herein (Figure 4). The simulated cement paste was assumed to have a 0.45 w/c ratio, which amounts to around 1300 kg/m^3 of cement (assuming specific gravity of 3.15).

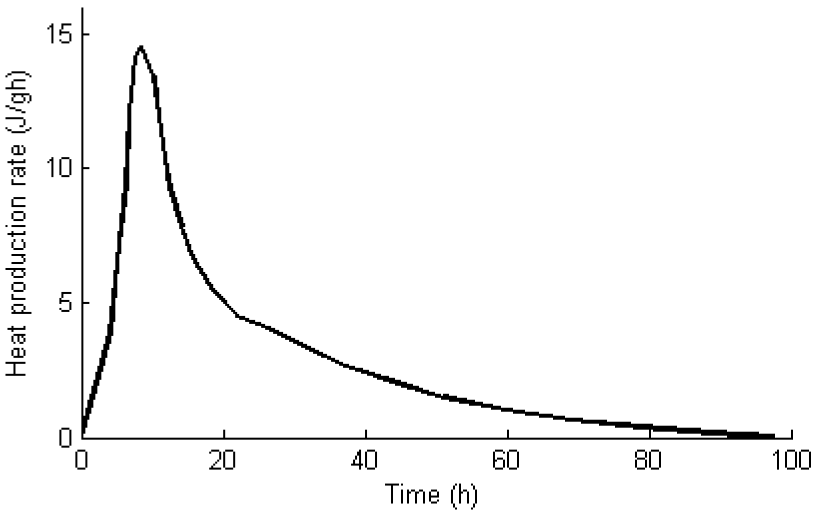

Figure 4. Heat production rate of Portland Cement CEM I 52.5 at 35 °C [50].

The measured heat production rate was first converted to volumetric heat production rate, and then applied as the source term according to equation (6).

For validation, a homogeneous 30x30x30 μm^3 lattice was generated. Cell size of 1x1x1 μm^3 with a sub-cell of 0.5x0.5x0.5 μm^3 was used for mesh generation (see Figure 1), with 27000 lattice nodes in total. Nodes at the domain edges were positioned exactly at the edge, in order to retain the total volume of the specimen (Figure 5). Adiabatic conditions were assumed (i.e. no heat exchange with the

[1] This particular heat production rate curve was selected due to its steep increase, because it may be assumed that concrete which exhibits a rapid heat evolution will have a higher risk of thermal cracking. In fact, any heat production curve, be it experimental (e.g. other curves in the paper of De Schutter and Taerwe [50]) or simulated (e.g. by HYMOSTRUC model [51, 52]), can be used in the model.

environment occurs)[2]. The initial temperature of the cement paste was assumed as 20°C (293.15K). According to the second law of thermodynamics, it is possible to predict the the temperature rise due to heat production as [29]:

$$\delta T = \frac{\delta Q \cdot MC}{\rho \cdot c_p} \tag{9}$$

where δT is the temperature difference caused by an increment in heat production δQ and MC the mass of cement. In figure 5, simulation results are compared with those obtained using equation (9).

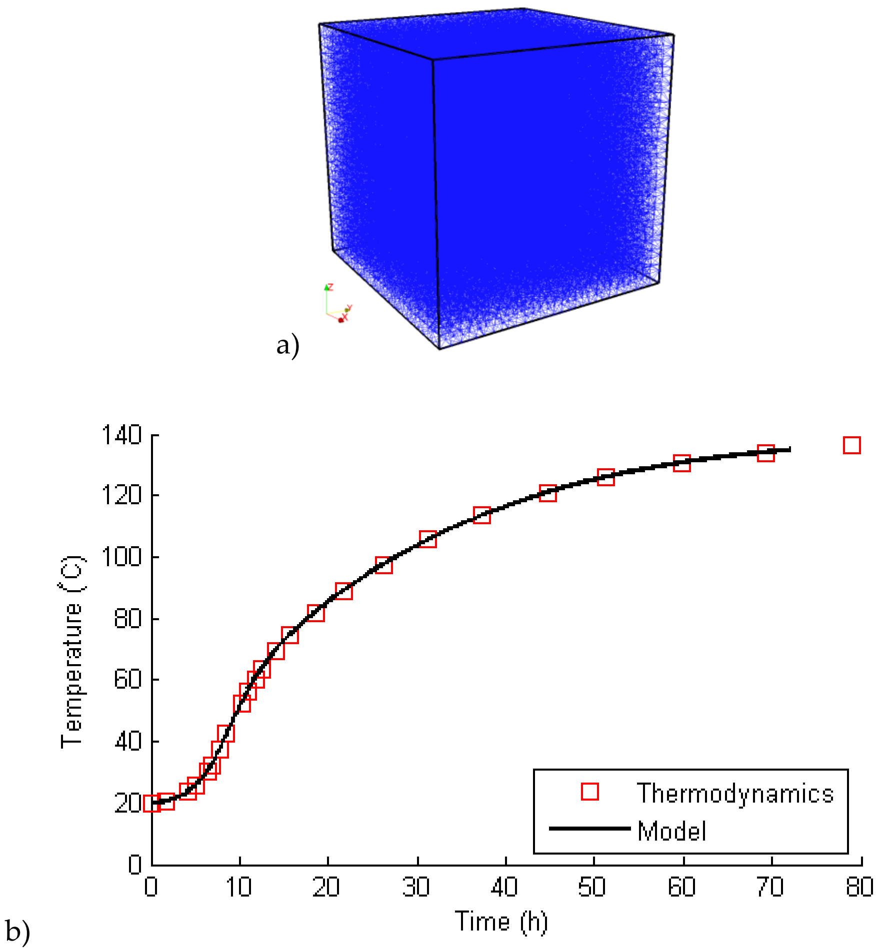

Figure 5. (a) A 30x30x30μm^3 random lattice used for model validation; (b) Comparison of the simulated temperature evolution and thermodynamic calculations

It can be seen in Figure 5 that there is no significant difference between the result of the lattice model and the theoretical (i.e. thermodynamics) solution. From this simple example, it can be concluded that the model does not show any significant numerical noise due to the lattice randomness.

[2] It should be noted that adiabatic tests are, in practice, performed mostly on concrete, not cement paste. In semi-adiabatic tests of Portland cement paste samples, temperatures close to 100°C have been recorded [53]. For comparison, a simulation of adiabatic temperature rise in concrete is given in the Appendix.

2.2. Structural modelling approach

Cracks in hardening concrete do not occur only due to material properties. Even more important is the structure itself [54]. Temperature induced deformations of a structure can be restrained by already hardened parts of the structure, leading to cracking. In that case, the rate of heating and cooling of the structure (together with the mechanical properties of the hardening material) will determine if cracking will occur.

On the structural scale, the influence of PCM additions on the risk of early-age cracking is assessed on the macro (i.e. structural) scale. Commercial finite element package FEMMASSE is used to simulate temperature evolution and stress distribution at this scale. FEMMASSE is a finite element model based on the state parameter concept [54, 55]. That means that the material properties are a function of the state of the material. The state can be maturity, degree of hydration, temperature, or moisture potential. On the macro scale, concrete is assumed to be homogeneous and isotropic (i.e. PCM microcapsules are not explicitly modelled). Instead, the heat absorbing capacity of PCM microcapsules in included in the concrete material.

2.2.1. Heat transport model

Heat transport in FEMMASSE is also simulated using equation 1. For the latent heat contribution during of the PCM material, also on this scale the heat capacity method is used [23, 49]:

$$\rho c_{p,c}(T)=\begin{cases}\rho c_{p,c} & \text{for } T<T_{pc}-\Delta T_{pc}/2\\ \rho c_{p,c}+\dfrac{h_f\cdot m_{pcm}}{\Delta T_{pc}} & \text{for } T_{pc}-\Delta T_{pc}/2\le T\le T_{pc}+\Delta T_{pc}/2\\ \rho c_{p,c} & \text{for } T>T_{pc}+\Delta T_{pc}/2\end{cases} \tag{10}$$

where $c_{p,c}$ is the specific heat capacity of concrete, and m_{pcm} the quantity of PCM microcapsules per cubic meter of the mixture. For simplicity, it was assumed that the addition of phase change microcapsules does not cause a change in density, thermal conductivity, or specific heat capacity (except due to the latent heat) of the hardening concrete.

3. Parametric studies

3.1.1. Material scale

In this section, physical and numerical parameters related to addition of PCM microcapsules are assessed on the meso-scale. In order to mimic the experiments, a part of the cement paste was replaced by PCM microcapsules. For simplicity, the microcapsules are considered to comprise only PCM, without a hard shell. This was done in order to minimize the computational effort, since in that case a much finer lattice mesh would need to be used. It is noted that an explicit consideration of a shell around the microcapsules would have a two-fold influence on the simulation result [49]: (1) it would reduce the total amount of PCM in the matrix (i.e. part of the capsule would be a non-phase change material); and (2) it would change the thermal properties of the matrix (due to different density, heat conductivity, and specific heat capacity of the shell material compared to the matrix). Nevertheless, the conslusions from the presented analyses are (in a qualitative sense) also valid for the “real” case.

In the following simulations it has been assumed that a part of the cement paste has been replaced by PCM microcapsules. Material properties used in the simulations are given in Table 1. Three replacement levels are considered: 10%, 20%, and 30% by volume of the cement paste. These replacement levels are realistic and in line with the work of Fernandes et al. [19]. For all the simulations in this section, the heat production rate presented in Figure 4 (obtained by De Schutter and Taerwe [50]), was used. Adiabatic heat evolution is also considered in this section, with all zero flux boundaries. Initial temperature was set to 20°C (293.15K).

In the work of Thiele et al. [31] it was shown that the packing arangement and polydispersity has no effect on the effective thermal properties of a composite material containing spherical particles. Therefore, in this study, three material structures with randomly distributed spherical microcapsules were created, for the 10%, 20%, and 30% replacement levels, respectively (Figure 6). These material structures were first voxelized and then overlapped on a lattice mesh (see Figure 2), creating a 2-phase composite lattice comprising PCM microcapsules and the cement paste.

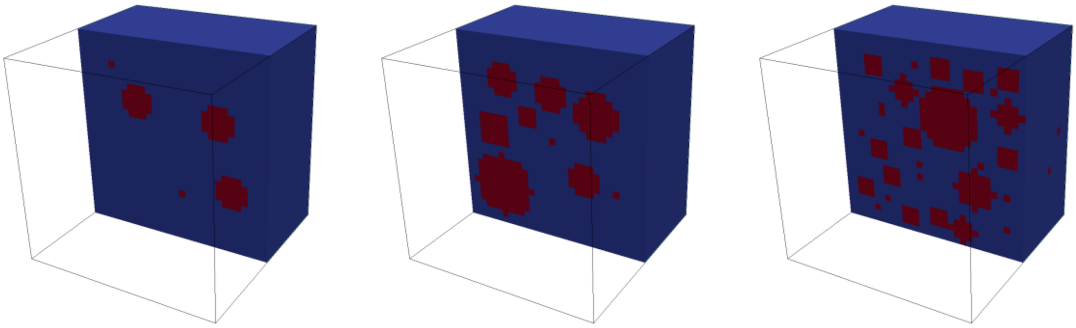

Figure 6. $30x30x30\mu m^3$ material structures comprising PCM microcapsules (cut in the middle to show PCM microcapsules) and cement paste with (left to right) 10%, 20%, and 30% PCM microcapsules per volume. PCM microcapsules are shown in red, while blue represents the cement paste matrix.

Because the heat production occurs only in the cement paste, the heat source term $\dot{Q}$ is applied only in the paste nodes. The phase change capsules have, therefore, a two-fold effect on the internal heat generation in the composite: first, they have a diluting effect due to the fact that they replace a part of the hydrating cement; and second, the phase change effect.

The diluting effect is considered first. This means that the heat absorbed by the system is only due to the sensible heat contribution. This essentially means that the PCM is considered simply as a filler material (e.g. limestone powder or fine sand) in terms of its thermal properties. It is simulated by considering the specific heat capacity of the PCM microcapsules to be constant (equation (7)). Temperature evolution for the three simulated PCM replacement levels (together with the reference cement paste) is given in Figure 7.

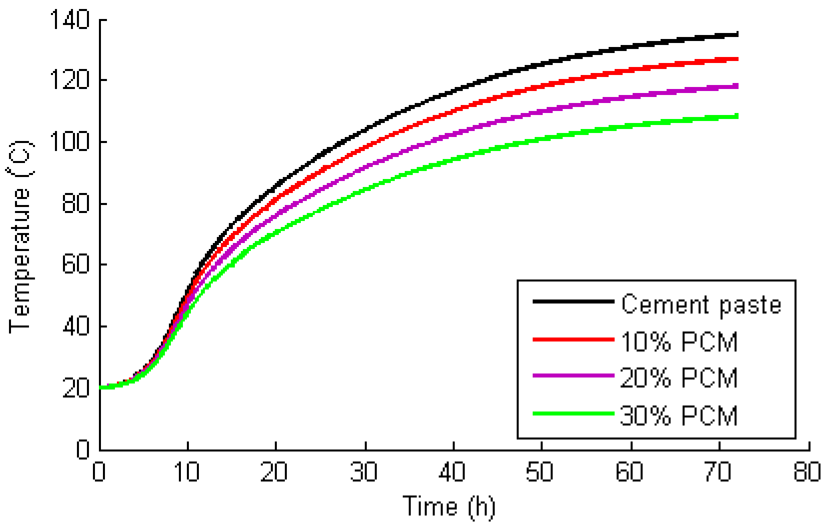

Figure 7. Simulated temperature evolution in a 30x30x30μm^3 microstructure containing different amounts of PCM microcapsules and without considering their latent heat contribution.

The diluting effect itself can be quite beneficial for the internal heat development, and is actually the only mechanism for cases when the initial temperature is higher than the phase change temperature. In the simulated example, the temperature achieved after 72 hours (3 days) of hydration was 134.8 °C, 127 °C, 118 °C, and 108.2 °C for the reference and 10%, 20%, and 30% PCM cases, respectively. This means that, by sensible heat only, the temperature can be reduced up to 26°C after three days in adiabatic test. It can be also noted that, in this case, the onset of temperature increase is not delayed: it is merely reduced due to less hydrating cement in the matrix. This is in accordance with semi-adiabatic tests performed by Thiele et al. [32]: they observed that, when the casting temperature was above the phase change temperature of the microcapsules (i.e. when only the sensible heat contribution of the PCM microcapsules is utilized), only a reduction in peak temperature resulted. The rate of temperature rise, however, remained similar.

Next, the latent heat contribution of the PCM microcapsules is also included. The phase change temperature is set as T_{pc}=25°C, the latent heat of fusion h_f=180 kJ/kg, and the temperature window as ΔT_{pc}=3°C. Temperature evolutions for the simulated meso-structures are shown in Figure 8.

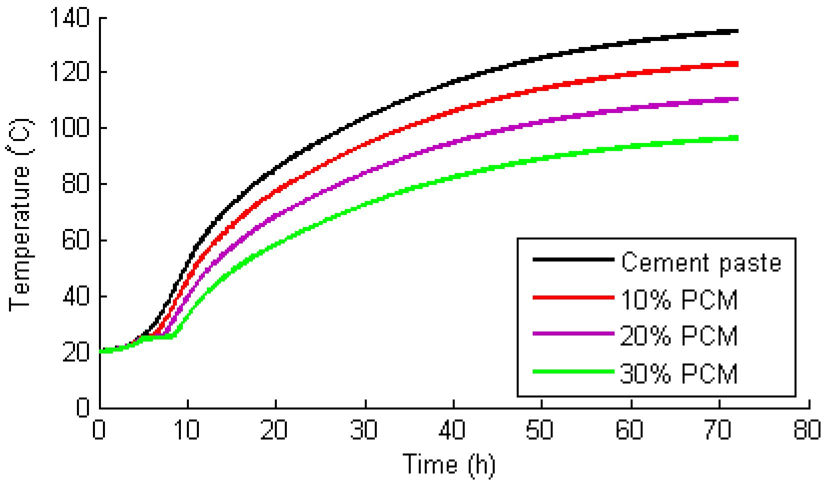

Figure 8. Simulated temperature evolution in a 30x30x30μm^3 microstructure containing different amounts of PCM microcapsules.

It can be seen that the phase-change capsules clearly delay the onset of temperature rise. The temperatures achieved after 72 hours are even lower in this case (compared to the case when only the sensible heat of PCM microcapsules is considered): 123.1 °C, 110.4 °C, and 96.4 °C. Figure 9 shows the latent heat contribution for all considered cases. Figure 10 illustrates the relation between the addition of microencapsulated PCMs and the adiabatic temperature rise.

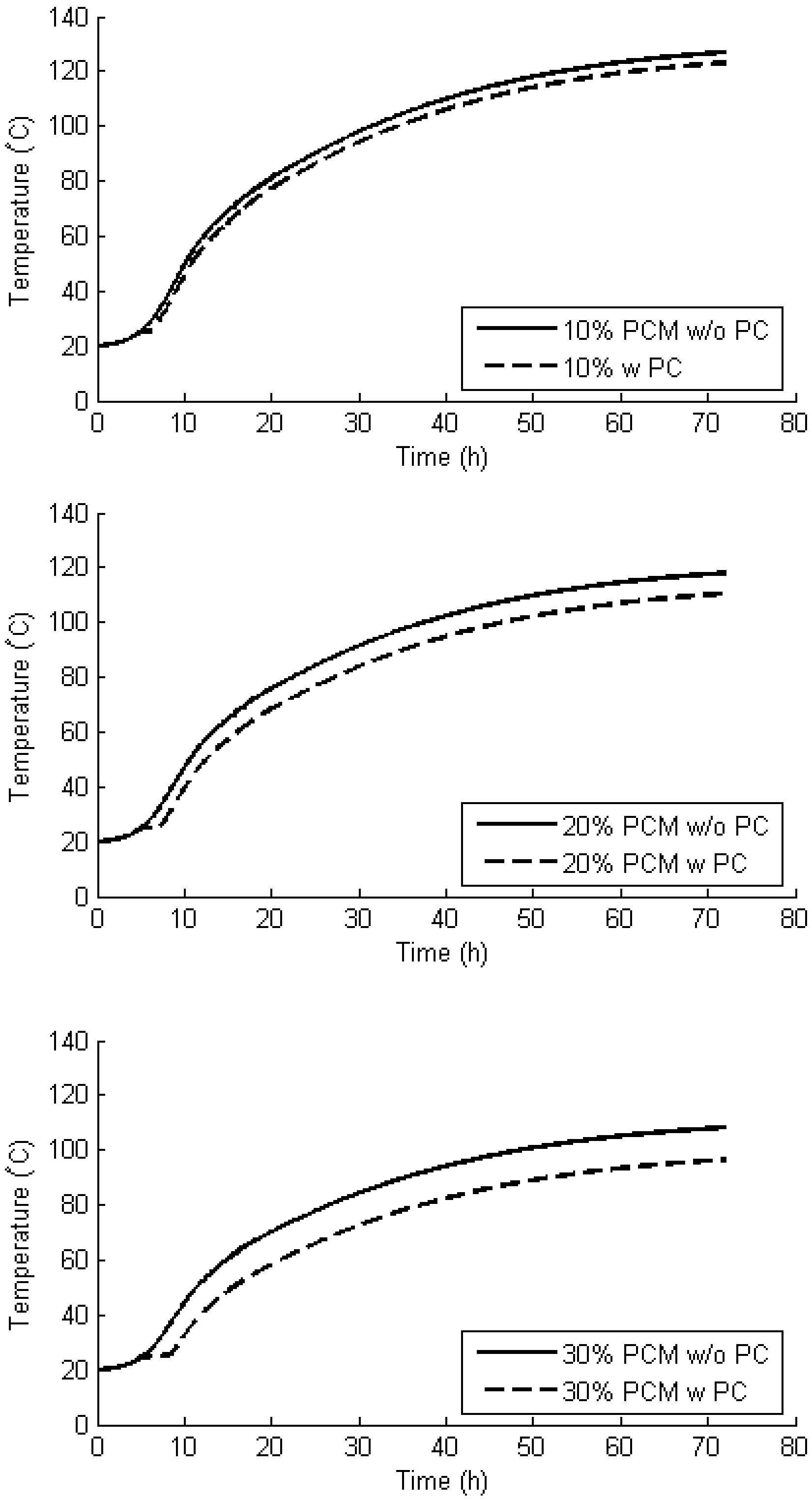

Figure 9. Influence of the latent heat contribution of PCM on the adiabatic temperature rise in cement paste containing different replacement levels of PCM microcapsules (w/o PC- without phase change, i.e. only diluting effect is considered; w PC- phase change, also phase change effect is considered).

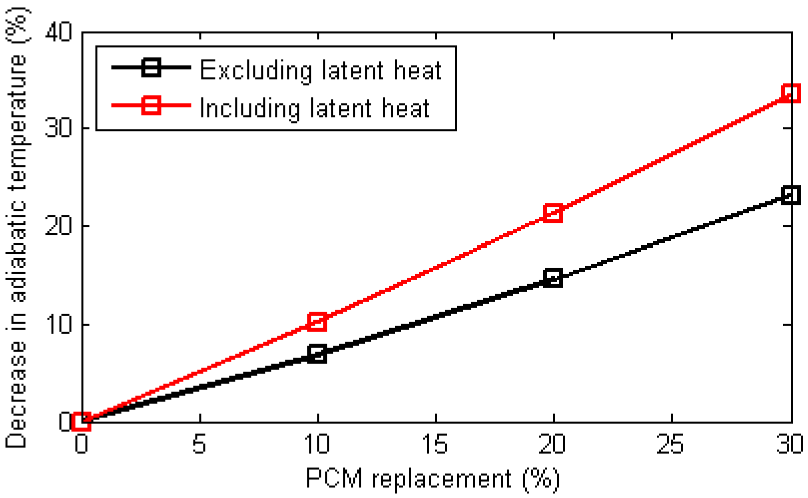

Figure 10. Decrease in simulated adiabatic temperature rise after 3 days of hydration with PCM microcapsules.

Clearly, the more PCM capsules there are, the more could be gained from their phase change in terms of delaying the temperature rise. The same trend was predicted by theoretical considerations of Qian et al. [18].

The ability of PCM microcapsules to absorb heat is highly dependent on their latent heat of fusion. Phase change materials with different latent heat of fusion (h_f) are available on the market [21]. In Figure 11, the influence of h_f on the adiabatic heat evolution for different replacement levels is explored. Note that most PCM materials proposed for temperature control in cementitious materials have h_f between 100-300 kJ/kg [17-19, 27, 49].

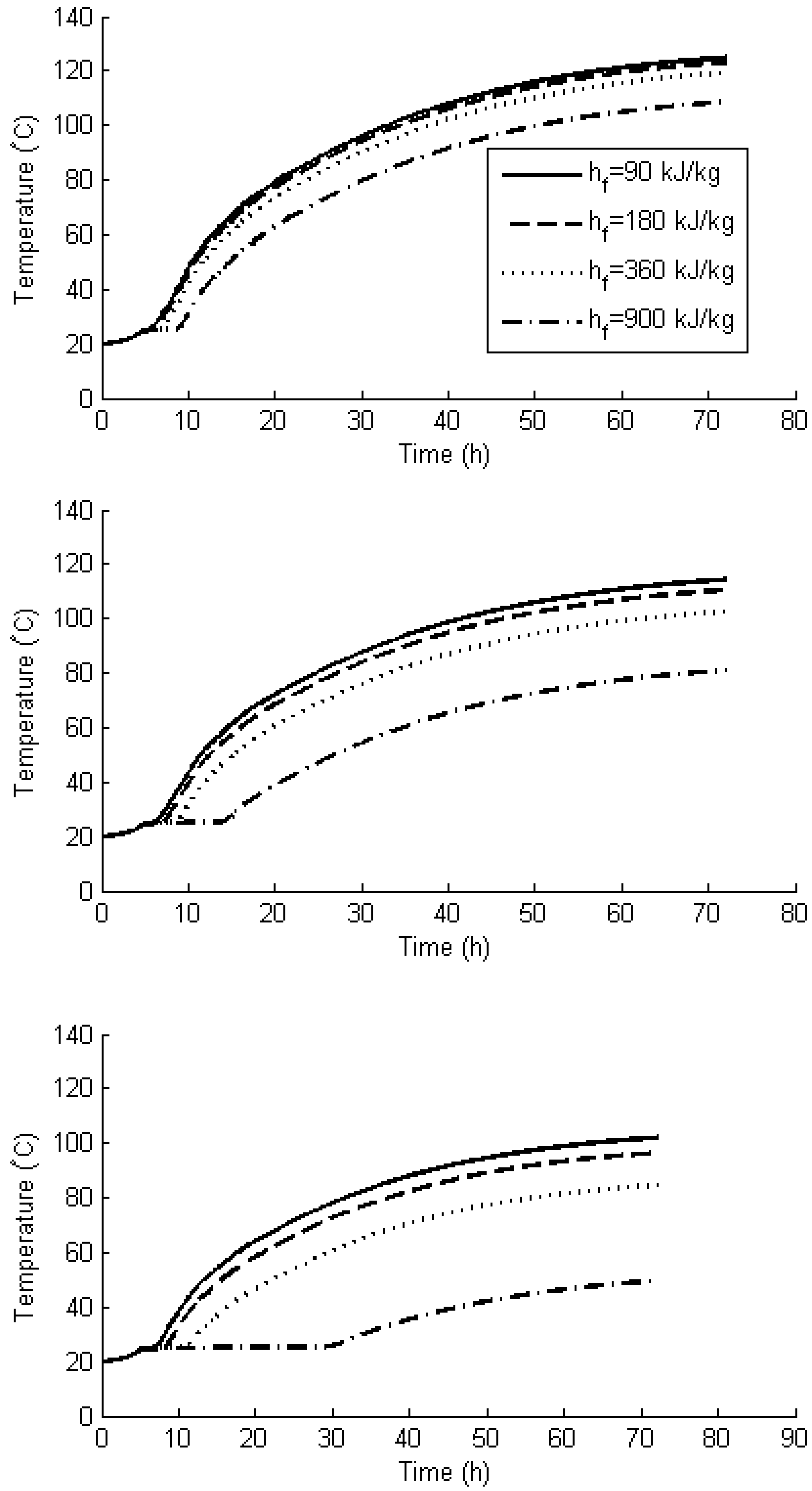

Figure 11. Influence of the latent heat of fusion of PCM microcapsules on the adiabatic temperature rise in cement paste containing different replacement levels (top to bottom: 10%, 20%, and 30% PCM microcapsules per volume).

In Figure 11 it can be seen that an increase in latent heat of fusion certainly has a great effect on the temperature development in adiabatic conditions. It needs to be observed that this increase becomes more beneficial as the total amount of PCM in the matrix increases. Therefore, a trade-off is possible between the amount of PCM and their latent heat capacity: lower amounts of PCMs with higher heat capacity can be used and vice versa, while the temperature development remains similar. However, it is desirable to use as low amount of PCM microcapsules as possible, since they could have a negative effect on the compressive [19, 29] and (to a lesser extent) tensile strength of concrete [19].

Another important aspect of using PCM microcapsules for control of thermal cracking is their phase change temperature. In Figure 12, a comparison of systems with three different phase change temperatures: 25°C, 35°C, and 45°C (with 10% PCM microcapsules and h_f=180kJ/kg).

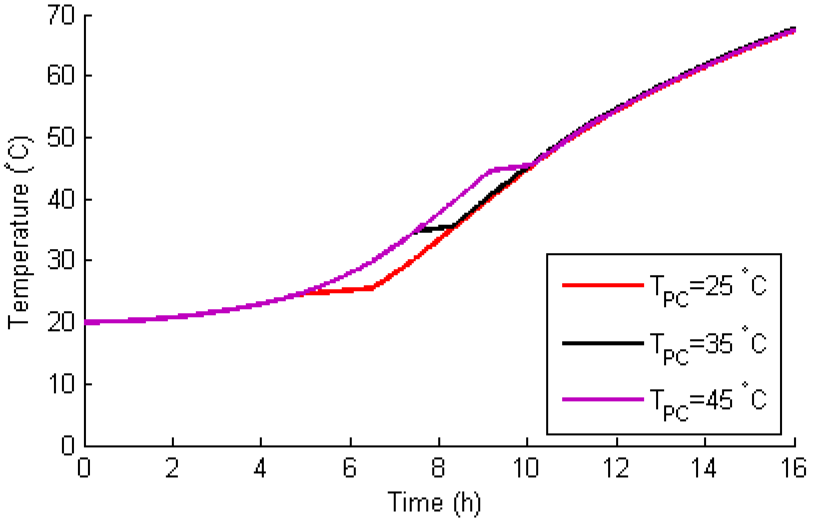

Figure 12. Influence of the phase change temperature of PCM microcapsules on the adiabatic temperature rise in cement paste containing different replacement levels.

It can be seen that the phase change temperature does not affect the final temperature in adiabatic conditions. In semi-adiabatic conditions (i.e. when some of the heat is lost to the environment), this may be somewhat different, as explored in the following section.

3.1.2. Structural scale

In this section, the influence of PCM microcapsule addition on temperature and stress development in hardening concrete wall is explored. As an example, a massive wall-slab system shown in Figure 13 is analysed. It is assumed in the analysis that the base slab has already hardened, and is restraining the thermal deformation occurring in the hardening wall. This is a typical scenario which could potentially lead to through cracking in the concrete wall.

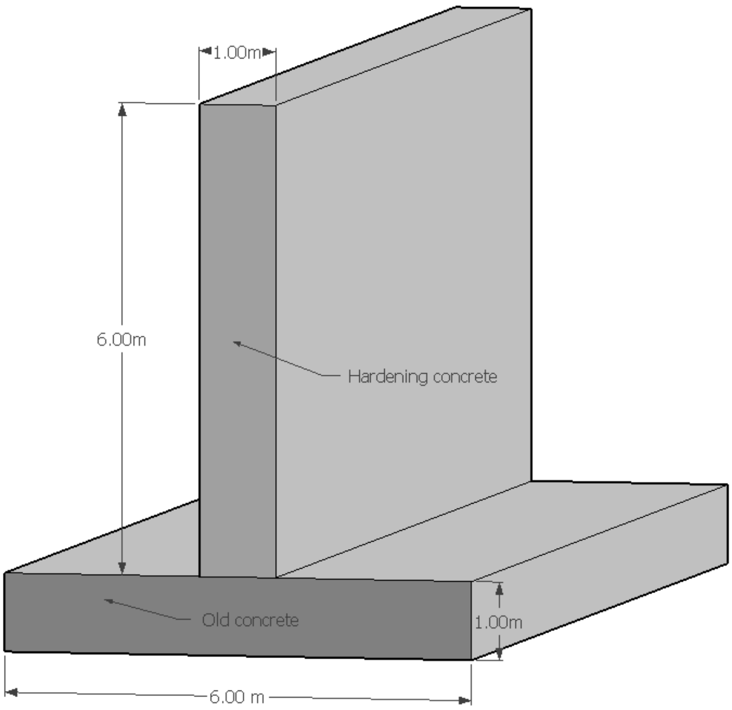

Figure 13. Geometry of the wall-slab system analysed in this section.

It is assumed further that the initial temperature of the base slab is 15°C, while the initial temperature of the young concrete is 20°C. The structure is exposed to the constant environmental temperature of 15°C. To simulate the heat exchange between the structure and the environment, convective boundary conditions are applied:

$$\overrightarrow{q_B} = a(T - T_e)_B \tag{11}$$

where $\overrightarrow{q_B}$ is the heat flux normal to the boundary B, a the heat transfer coefficient, and T_e the temperature of the environment. For all simulations in this section, heat of hydration as shown in Figure 14 is used.

Convective boundary conditions are applied on all surfaces of the structure. The hardening concrete is covered by 18mm plywood plate formwork. Wind speed is assumed to be 5 m/s, which together with the formwork results in a heat transfer coefficient of 7 W/m^{2}K. Meanwhile, the base slab is directly exposed to the wind, resulting in a heat transfer coefficient of 25 W/m^{2}K. The formwork is removed after 4 days, and the whole structure is then directly exposed to the environment, with a heat transfer coefficient of 25 W/m^{2}K.

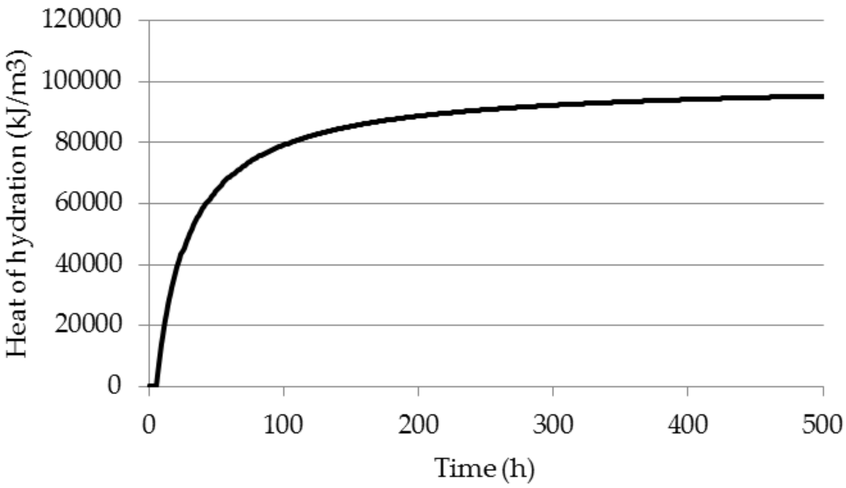

Figure 14. Development of heat of hydration of hardening concrete used in macro-scale simulations.

Two-dimensional simulations of the wall-slab system are performed, using the plane strain theory which is applicable since the out-of-plane dimension (i.e. length) is much larger than the cross-section of the structure. Mechanical properties of the hardening concrete are maturity dependent, as given in Figure 15. Other properties used in the analyses are given in Table 2. Note that influence of PCM microcapsules on mechanical properties of concrete and their development has been neglected in the present simulations: although it is known that the PCM microcapsules cause a reduction in the compressive strength of concrete [29], they affect the elastic modulus and the tensile/bending strength to a lesser extent [19]. These effects will be considered in the model once more data is available.

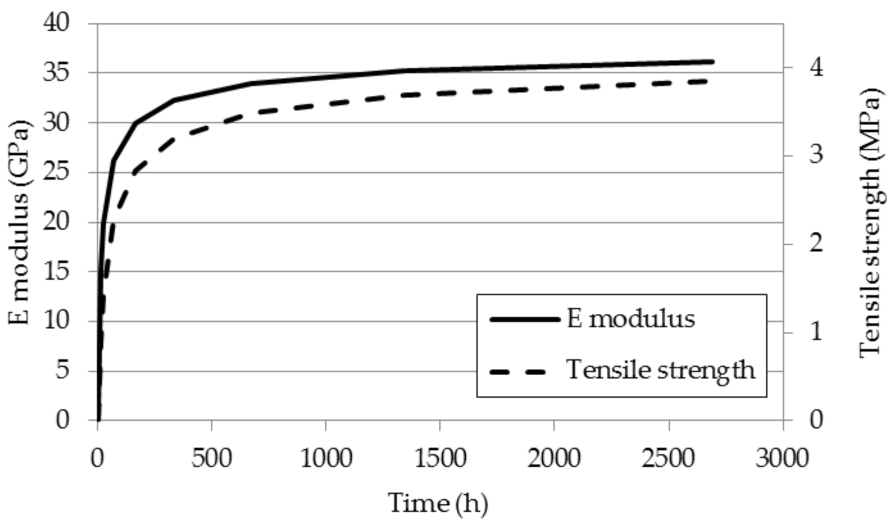

Figure 15. Development of E modulus and tensile strength of hardening concrete used in macro-scale simulations.

Table 2. Material properties used in macro-scale simulations.

	Material property	Value
Hardening concrete (wall)	Compressive strength at 28 days	43 MPa
	Tensile strength at 28 days	3.50
	Young's modulus at 28 days	34 Gpa
	Poisson's ratio	0.2
	Coefficient of thermal expansion	$1 \cdot 10^{-5}$ 1/°C
	Density	2300 kg/m^3, ref. [49]
	Thermal conductivity	1.4 W/mK , ref. [49]
	Specific heat capacity	880 kJ/kgK, ref. [49]
Old concrete (slab)	Thermal conductivity	2.4 W/mK
	Specific heat capacity	1000 kJ/kgK

The wall/slab system is discretized using fully integrated four node finite elements using the plane strain formulation [56]. In total, 1000 elements and 1111 nodes were used in all analyses (Figure 16). The analyses were carried out for 500 hours with a time step of 0.25 hours and storage of the results at every 0.5 hours. Time dependent behaviour of concrete (creep and shrinkage) were not considered.

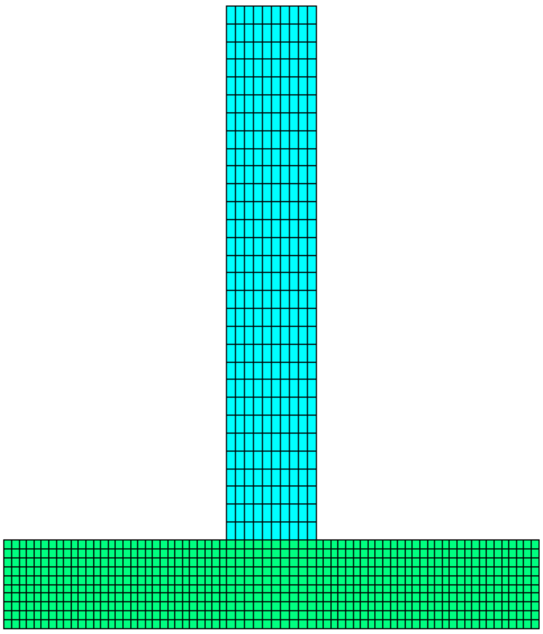

Figure 16. Two dimensional finite element mesh used for simulations in this section. Hardening concrete is shown as light blue, while the base slab is shown as green.

First, the influence of PCM microcapsule addition on temperature and stress development in hardening concrete is simulated. Four different addition levels are simulated: 0, 30, 60, and 90 kg/m^3 of microencapsulated PCM. Note that these addition levels are realistic and in line with existing literature: for lightweight aggregates impregnated with PCM, addition levels of 50-120 kg/m^3 have been suggested by Sakulich and Bentz [27] as optimum and maximum quantity of PCM in concrete, respectively, while Farnam et al. [26] used even higher quantities (150 kg/m^3); for microencapsulated PCM in concrete, Hunger et al. [29] used 23-113 kg/m^3. In these simulations, h_f=180 kJ/kg [49] and phase change temperature of 25°C are used. Development of maximum temperature and out-of-plane stress for these simulations is shown in Figure 17 and Figure 18.

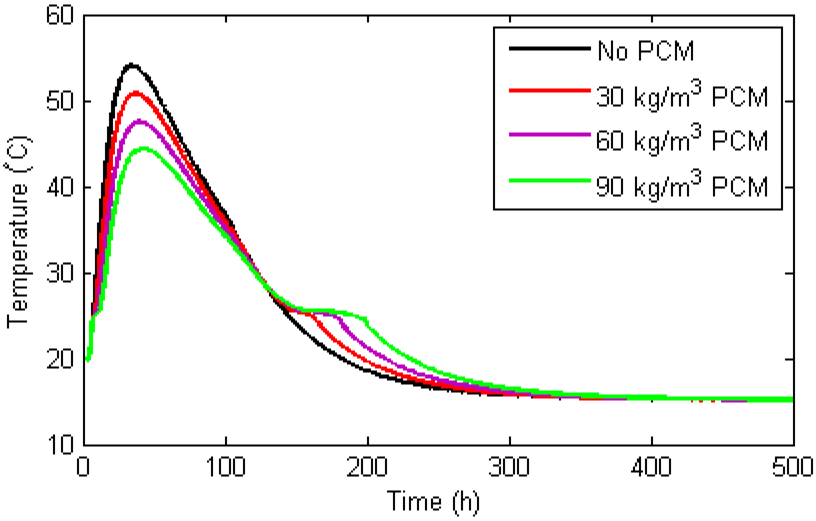

Figure 17. Simulated development of maximum temperature in a hardening concrete wall depending on the PCM microcapsule addition level.

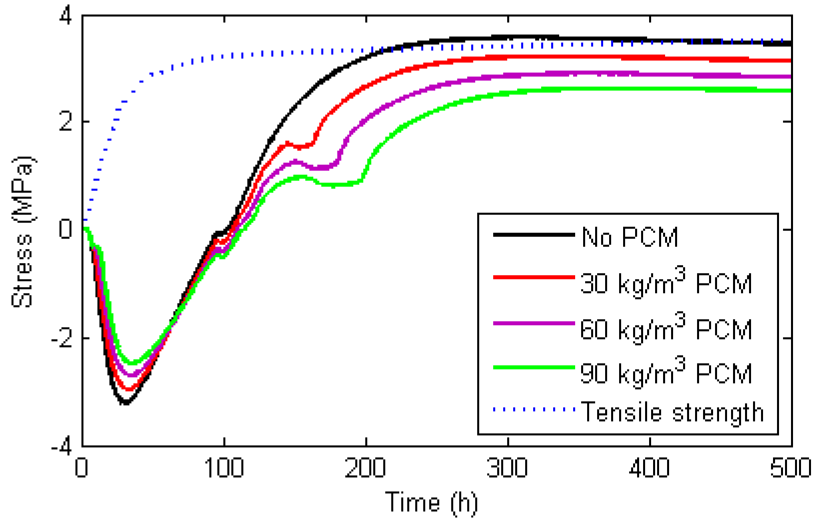

Figure 18. Simulated development of out-of-plane stress in a hardening concrete wall depending on the PCM microcapsule addition level.

In Figure 17, it can be seen that, as already shown by the meso-scale model (section 3.1.1), the PCM microcapsule addition delays the onset of temperature rise. Combined with loss of heat to the environment, this results in a lower maximum temperature with increasing PCM addition level. Furthermore, the onset of maximum temperature is delayed (Table 3). It is also important that PCM addition slows down the cooling phase, with increasing PCM levels resulting in a smoother temperature curve. This has implications on the stress development in the hardening wall, as shown in Figure 18. First, the temperature increase results in occurrence of compressive stresses. The magnitude of these stresses decreases with the increase in PCM content. However, this phase is not critical for crack development in the hardening wall: it is the cooling down phase that results in tensile stresses. In this phase, the PCM addition results in a decrease of tensile stresses in the wall. By comparing the tensile stresses with the tensile strength of the concrete, it is clear that, when no measures are taken, cracking will occur. Already when 30 kg/m^3 of PCM is used, the stresses are lower than the tensile strength. These stresses also occur at a later instance compared to the reference case (Table 3). Further increase in PCM content causes an even larger drop in tensile stress. There are two additional points that need to be stressed again here: on the one hand, the influence of PCM addition on the tensile strength is not taken into account, and it may be the case that the actual tensile strength of the PCM concrete is somewhat lower; on the other hand, the influence of PCM on thermal properties and the dilution effect (section 3.1.1) is also not taken into account, which may result in even lower stresses. Therefore, these two opposing effects may to a certain extent affect the results.

Next, the influence of phase change temperature of PCM microcapsules is explored. In section 3.1.1, it was shown that the temperature of phase change does not have any influence on the maximum temperature occurring in an adiabatic test. In the structural test, however, part of the heat is lost to the environment, and the influence of phase change temperature is possibly different. In these simulations, h_f=180 kJ/kg [40] and 90 kg/m^3 of PCM is assumed. Development of maximum temperature and out-of-plane stress for these simulations is shown in Figure 19 and Figure 20.

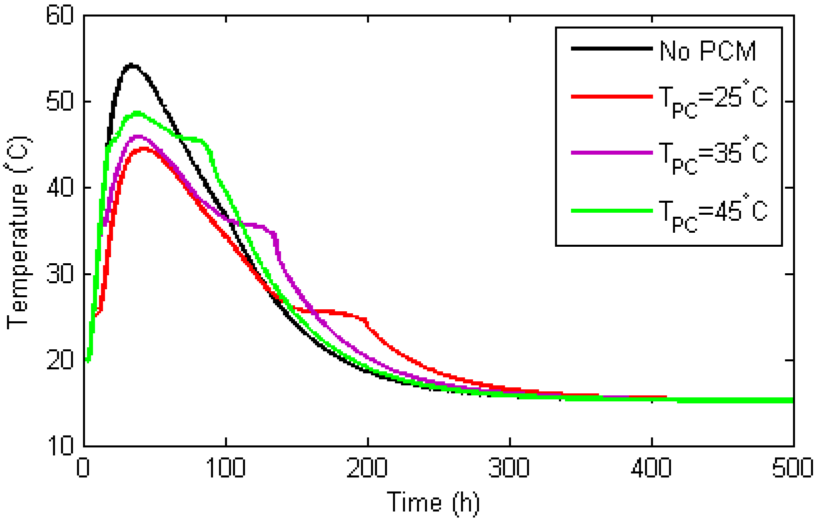

Figure 19. Simulated development of maximum temperature in a hardening concrete wall depending on the phase change temperature of PCM microcapsules.

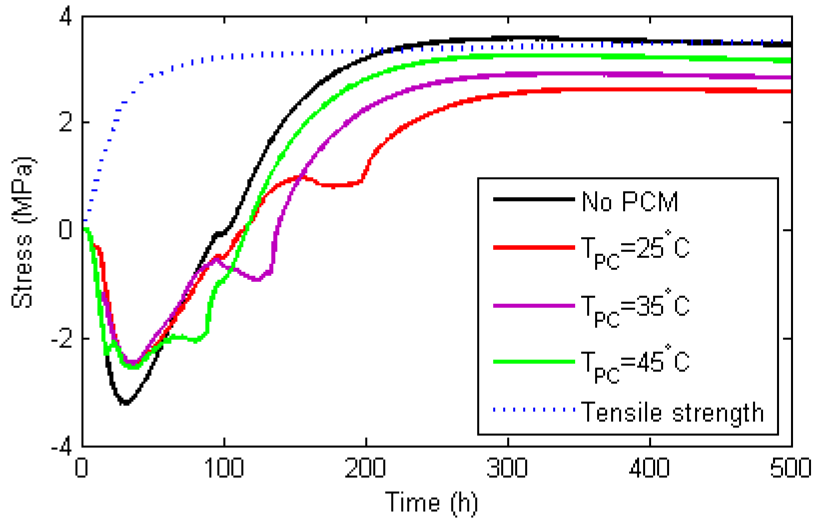

Figure 20. Simulated development of out-of-plane stress in a hardening concrete wall depending on the phase change temperature of PCM microcapsules.

Three different phase change temperatures are explored: 25°C, 35°C, and 45°C. It can be seen in Figure 19 that lower PCM temperatures result in lower maximum temperature (for the assumed casting temperature of 20°C and the assumed material and environmental parameters). The cooling-down phase shows a similar behaviour: the highest phase change temperature prolongs the cooling down phase less than the lowest phase change temperature. This results in marked differences in maximum tensile stress that occurs in this phase: for the lowest phase change temperature, lowest stresses occur and at the later stage (Figure 20 and Table 3). This will result in a lower probability of thermal cracking.

Finally, the influence of heat of fusion of PCM microcapsules is explored. Similar to the meso-scale model in section 3.1.1., heats of fusion ranging from 90-900 kJ/kg were explored. In this set of simulations, 90 kg/m^3 of PCM was assumed with a phase change temperature of 25°C. Development of maximum temperature and out-of-plane stress for these simulations is shown in figures 21 and 22.

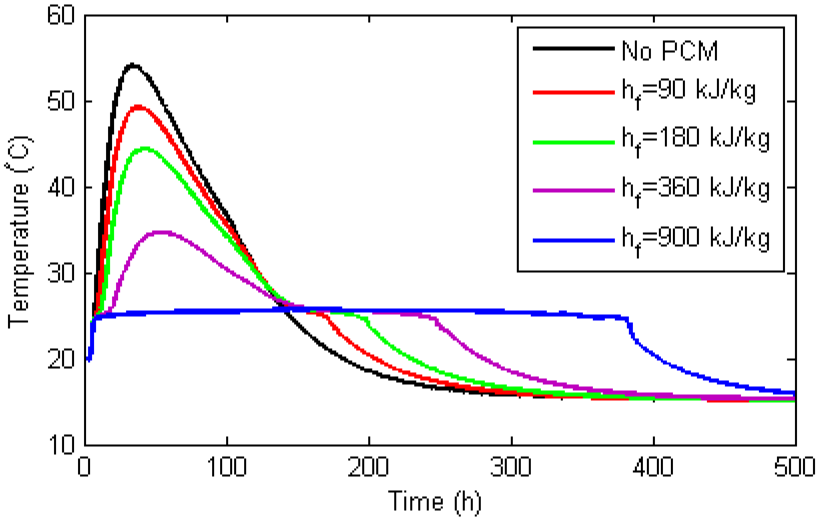

Figure 21. Simulated development of maximum temperature in a hardening concrete wall depending on the heat of fusion of PCM microcapsules.

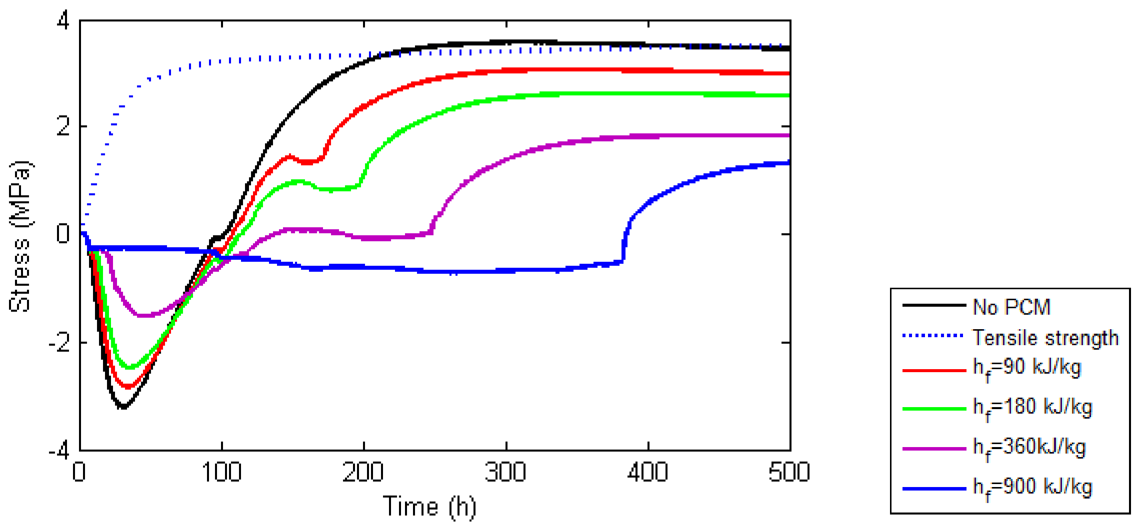

Figure 22. Simulated development of out-of-plane stress in a hardening concrete wall depending on the heat of fusion of PCM microcapsules.

As expected and in accordance with the meso-scale model, the increase in heat of fusion of PCM microcapsules causes a decrease in maximum temperature (Figure 21). Furthermore, it prolongs the cooling phase. In the extreme case of h_f=900 kJ/kg (which is probably not feasible in practice), there is hardly any increase in temperature (about 5°C, Table 3). Tensile stresses occurring in the cooling down phase decrease with the increase in heat of fusion (Figure 22). It needs to emphasized again here that a trade-off between the heat of fusion and quantity of PCM microcapsules is possible, and that use of a smaller quantity of PCM microcapsules with high heat of fusion is desirable in order to minimize the loss of mechanical properties.

Table 3. Summary of the macro-scale simulation results.

In common	Analysis	Max temperature (°C)	Occurring at (h)	Max stress (MPa)	Occurring at (h)
T_{pc}=25°C, h_f=180 kJ/kg	No PCM	54	34.5	3.56	302
	30 kg/m^3	50.76	37	3.21	331.5
	60 kg/m^3	47.47	39.5	2.89	347
	90 kg/m^3	44.34	42	2.62	372
90 kg/m^3, h_f=180 kJ/kg	T_{pc}=35°C	45.77	38.5	2.91	334.5
	T_{pc}=45°C	48.46	38.5	3.25	315
90 kg/m^3, T_{pc}=25°C	h_f=90 kJ/kg	49.17	38.5	3.06	339
	h_f=360 kJ/kg	34.68	54	1.83	434.5
	h_f=900 kJ/kg	25.75	164	1.32	500

It should be stressed that the quantitative findings of the presented analyses are limited by the assumptions adopted. For example, if the environment would be warmer, it is possible that the optimal temperature of phase change would be different than the one found for the considered conditions. Furthermore, it is possible that, in certain cases, it would be desirable to combine the use of PCM microcapsule addition with traditional measures for control of thermal cracking, such as decrease of casting temperature through use of ice [54]. The model presented is versatile and different input parameters and measures can be considered and combined. In the future, the model will be applied for simulating large-scale experiments related to control of temperature rise and thermal cracking through use of PCM microcapsules.

4. General discussion

Simulations considering the material on the meso-scale (section 3.1.1) have releveled several important aspects related to use of microencapsulated phase change materials to reduce temperature rise in cement paste. PCM microcapsules reduce the temperature through a synergy of two mechanisms: the dilution effect and the capture of heat through phase change. It should be noted that the former does not delay the onset of temperature rise, while the latter does. It was also shown that he higher the amount of PCM microcapsules, the longer the temperature rise will be delayed. The same goes for the latent heat of fusion: the higher the latent heat of fusion of PCM microcapsules, the later the temperature rise will occur. It can be inferred that a trade-off between these two factors is possible. Note that use of a lower amount of PCM microcapsules with high latent heat of fusion is beneficial from a structural point of view, since the decrease of (compressive) strength has shown to be proportional to the PCM addition in cement paste [19], although this is not always the case for mortar and concrete [57]. Finally, it was shown that the phase change temperature (T_{PC}) does not influence the adiabatic temperature rise. This means that, depending on the environmental conditions expected, the phase change temperature of microencapsulated PCMs can be tailored without affecting the maximum (theoretical) temperature which may occur.

Full-scale (structural) simulations (section 3.1.2) have focused on the interaction between the hardening concrete structure, external restraints, and the environment. Building up on the meso-scale analysis, the aim of this section was to prove that the decrease in temperature rise due to addition of microencapsulated PCMs can reduce the maximum tensile stress occurring in the structure. It was shown by the simulations to be possible, even for relatively low amounts of considered PCM microcapsules (30kg/m^3). The main contribution to stress reduction seems not to come from the reduced peak temperature, but from the prolonged period of cooling down compared to the case when no PCMs are added to the mix. This means that the temperature difference between different parts of the structure are lowered, leading to lower stresses. In addition, the occurrence of maximum tensile stress is delayed in proportion to the PCM addition (or the latent heat of fusion), meaning that the time dependent mechanical properties (most pertinent being the tensile strength in this case) will be higher, thereby further reducing the risk of cracking. Furthermore, full-scale simulations showed a significant influence of the phase change temperature (T_{PC}) on temperature and stress development. This means that PCMs need to be tailored for expected environmental conditions.

Several important aspects have been neglected in the present work for simplicity. In meso-scale simulations, the existence of a hard shell around PCM was neglected, and the microcapsules were considered to comprise pure phase change material. The existence of a (polymeric) hard shell would, to a certain extent, influence the thermal properties of the considered composite. Furthermore, it would reduce the effective amount of the PCM (for a given microcapsule volume) and thus the total heat storage capacity. In full-scale simulations, also, it was assumed that the PCM addition does not affect the density, thermal conductivity, or the specific heat capacity of concrete. This may, to a certain extent, affect the temperature distribution in the considered structure. Probably the most important simplification in the full-scale model was neglecting the influence of the PCM microcapsule addition on the mechanical properties of concrete. Although it was found that addition of a significant percentage of PCM can have a negative effect on compressive and tensile strength [19, 29, 58], the fracture toughness remains largely intact [19]. Furthermore, the addition of compliant inclusions may increase the creep and relaxation of the hardening concrete [59], thereby reducing the stresses. Finally, it was implicitly assumed that the all PCM microcapsules added to the mix will survive the mixing process and remain intact. However, it is possible that some PCM microcapsules break during the mixing of the concrete [19, 58]. If this would happen, it is possible that chemical reactions between the PCM and the hydration products would occur. For example, Farnam et al. [26] found that methyl laureate reacts with the cementitious matrix causing an expansive reaction and cracking of the mortar. All these aspects will be considered in the future when more experimental data is available.

5. Summary and conclusions

In this work, the influence of phase change materials (PCMs) addition (in the form of microcapsules) on hydration temperature evolution and stress development in hardening concrete is studied using numerical models. First, addition of discrete microcapsules is considered on the meso-scale (i.e. cement paste level) using the lattice model. The influence of PCM percentage, phase change temperature, and latent heat of fusion on the adiabatic temperature development is studied on this scale. Meso-scale simulations have revealed the following:

- The addition of PCM microcapsules in cement paste reduces the adiabatic heat rise through two mechanisms. First, the sensible heat contribution (together with the diluting effect) can reduce the total heat rise, without affecting the onset of the temperature rise. Second, the latent heat contribution will delay the onset of temperature rise.

- The latent heat contribution becomes more dominant as the percentage of PCM microcapsules increases. This can be exploited by increasing the latent heat of fusion of the PCM microcapsules.
- The phase change temperature of PCM microcapsules does not affect the heat rise in an *adiabatic* test.

Additionally, a commercial FE package is used on the macro-scale (i.e. concrete level) to study the behaviour of a structural system comprising a hardening wall on a slab. The influence of PCM addition, phase change temperature, and latent heat of fusion on the semi-adiabatic temperature rise and stress development in the hardening wall is explored. Based on the structural-scale analyses, the following conclusions can be drawn:

- In *semi-adiabatic* (i.e. field) conditions, the addition of PCM in hardening concrete has potential to delay the temperature rise, reduce the maximum tensile stress, and delay its occurrence. The maximum tensile stress is inversely proportional to the amount of PCM added to the mix.
- In *semi-adiabatic* conditions, the phase change temperature does influence the maximum temperature developing in the structure. In the considered example, the lowest phase change temperature (25°C) resulted in the lowest maximum temperature. Furthermore, it also resulted in the lowest magnitude of tensile stresses occurring at a later time compared to other simulated phase change temperatures. Consequently, it has the lowest probability of cracking. Note that this is related to the environmental conditions, and that the PCMs may need to be tailored depending on the climate.
- An increase in the latent heat of fusion serves the same purpose as an increase in PCM addition: it lowers the maximum temperature and maximum stress, and delays their occurrence. Especially the cooling phase is prolonged. Therefore, a trade-off between the heat of fusion and quantity of PCM microcapsules is possible, where a smaller amount of PCMs with a higher heat of fusion can be used with the same (thermal) efficiency. This would be beneficial also in terms of mechanical properties of the concrete.

The present paper clearly proves that, in theory, properly designed cementitious materials with incorporated microencapsulated PCMs have potential to reduce heat evolution and thus mitigate early age thermal cracking. There are numerous issues that need to be addressed before this can be done in engineering practice. First, proper encapsulation of PCM is essential: microcapsules need to be hard enough to sustain mixing and pouring of the concrete, and stable in a highly alkaline environment of concrete for longer periods of time. Second, if it intended that the same microcapsules be used to reduce thermal fatigue of concrete, it is necessary that the PCM material itself is stable and that it can sustain numerous solid-to-liquid transitions (and vice versa) without losing its latent heat storing ability. And third, for structural applications, it is important that these relatively soft and compliant inclusions do not affect strength, creep, and shrinkage to very high extents. All of these issues need to be addressed prior to fully recommending the use of microencapsulated PCMs in engineering practice. This will form a basis of the experimental part of the current research project and will be studied in the near future.

Acknowledgements

The authors would like to acknowledge the financial support by the EU-Infravation (An Infrastructure Innovation Programme) for the project ECLIPS – Enhancing Concrete Life in Infrastructure Through Phase-change systems.

Appendix

In order to assure that the meso-scale model provides realistic results in terms of adiabatic temperature rise, here an adiabatic experiment performed on concrete is simulated. The same 30x30x30 μm^3 specimen as in section 2.1.2 is used with the heat production rate given in figure 6. The concrete mixture used by De Schutter and Taerwe is used [50], with 300 kg/m^3 of cement and unit weight of 2400 kg/m^3. The specific heat capacity was set to 1000 kJ/kg, and the initial temperature to 20°C. Figure 23 gives the theoretical (thermodynamics) temperature rise and that calculated using the meso-scale model. It can be seen that the model shows a realistic rise of temperature, and that it matches the thermodynamic calculations quite well.

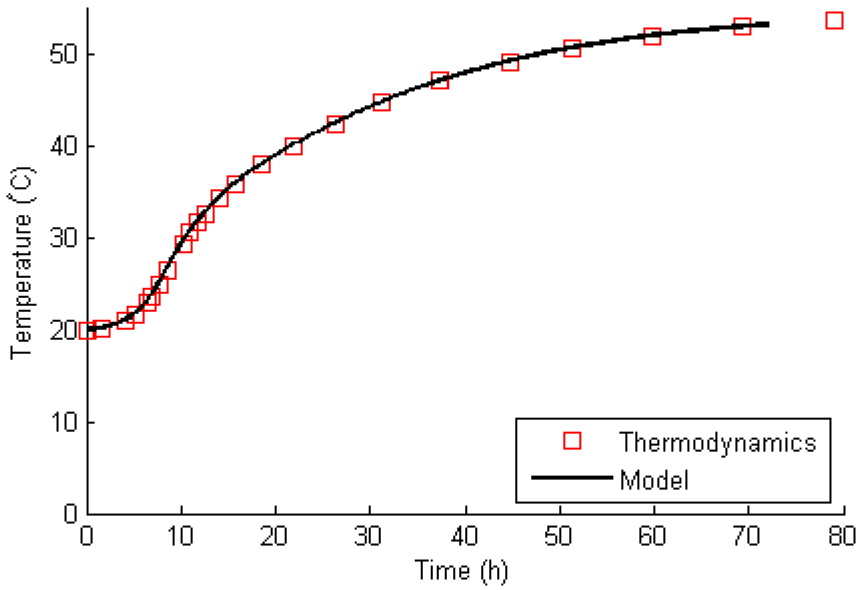

Figure 23. Comparison of the simulated temperature evolution and thermodynamic calculations for concrete.

References:

[1] Emborg M, Bernander S. Assessment of risk of thermal cracking in hardening concrete. Journal of Structural Engineering. 1994;120(10):2893-912.

[2] De Schutter G. Finite element simulation of thermal cracking in massive hardening concrete elements using degree of hydration based material laws. Computers & Structures. 2002;80(27):2035-42.

[3] Yuan Y, Wan Z. Prediction of cracking within early-age concrete due to thermal, drying and creep behavior. Cement and Concrete Research. 2002;32(7):1053-9.

[4] Mehta PK, Monteiro PJ. Concrete: microstructure, properties, and materials: McGraw-Hill New York; 2006.

[5] Waller V, d'Aloïa L, Cussigh F, Lecrux S. Using the maturity method in concrete cracking control at early ages. Cement and Concrete Composites. 2004;26(5):589-99.

[6] Bolander JE, Kim K, Sasaki K. Thermal effects on early-age cracking potential of concrete bridge decks. In: Bićanić N, Mang H, Meschke G, de Borst R, editors. Computational Modelling of Concrete Structures. St. Anton am Arlberg: CRC Press; 2014. p. 723-9.

[7] ACI. Cement and Concrete Terminology (ACI 116R-00). USA: American Concrete Institute Pubs; 2000.

[8] Gajda J, Vangeem M. Controlling temperatures in mass concrete. Concrete international. 2002;24(1):58-62.

[9] Malhotra VM, Ramezanianpour A. Fly ash in concrete: Canmet; 1994.

[10] Atiş CD. Heat evolution of high-volume fly ash concrete. Cement and Concrete Research. 2002;32(5):751-6.

[11] Šavija B, Schlangen E, Pacheco J, Millar S, Eichler T, Wilsch G. Chloride ingress in cracked concrete: a laser induced breakdown spectroscopy (LIBS) study. Journal of Advanced Concrete Technology. 2014;12(10):425-42.

[12] Kwon SJ, Na UJ, Park SS, Jung SH. Service life prediction of concrete wharves with early-aged crack: Probabilistic approach for chloride diffusion. Structural Safety. 2009;31(1):75-83.

[13] Blagojević A. The Influence of Cracks on the Durability and Service Life of Reinforced Concrete Structures in relation to Chloride-Induced Corrosion: A Look from a Different Perspective: TU Delft, Delft University of Technology; 2016.

[14] Nobuhiro M, Kazuo U. Nonlinear thermal stress analysis of a massive concrete structure. Computers & Structures. 1987;26(1):287-96.
[15] Pane I, Hansen W. Investigation of blended cement hydration by isothermal calorimetry and thermal analysis. Cement and Concrete Research. 2005;35(6):1155-64.
[16] Kim JK, Kim KH, Yang JK. Thermal analysis of hydration heat in concrete structures with pipe-cooling system. Computers & Structures. 2001;79(2):163-71.
[17] Bentz DP, Turpin R. Potential applications of phase change materials in concrete technology. Cement and Concrete Composites. 2007;29(7):527-32.
[18] Qian C, Gao G, Zhu C, Guo Z. Influence of phase change materials on temperature rise caused by hydration heat evolution of cement-based materials. Magazine of Concrete Research. 2010;62(11):789-94.
[19] Fernandes F, Manari S, Aguayo M, Santos K, Oey T, Wei Z, et al. On the feasibility of using phase change materials (PCMs) to mitigate thermal cracking in cementitious materials. Cement and Concrete Composites. 2014;51:14-26.
[20] Qian C, Gao G. Reduction of interior temperature of mass concrete using suspension of phase change materials as cooling fluid. Construction and Building Materials. 2012;26(1):527-31.
[21] Zalba B, Marín JM, Cabeza LF, Mehling H. Review on thermal energy storage with phase change: materials, heat transfer analysis and applications. Applied thermal engineering. 2003;23(3):251-83.
[22] Hawes D, Banu D, Feldman D. Latent heat storage in concrete. II. Solar energy materials. 1990;21(1):61-80.
[23] Lamberg P, Lehtiniemi R, Henell A-M. Numerical and experimental investigation of melting and freezing processes in phase change material storage. International Journal of Thermal Sciences. 2004;43(3):277-87.
[24] Snoeck D, Priem B, Dubruel P, De Belie N. Encapsulated Phase-Change Materials as additives in cementitious materials to promote thermal comfort in concrete constructions. Materials and Structures. 2016;49(1):225-39.
[25] Ling T-C, Poon C-S. Use of phase change materials for thermal energy storage in concrete: an overview. Construction and Building Materials. 2013;46:55-62.
[26] Farnam Y, Krafcik M, Liston L, Washington T, Erk K, Tao B, et al. Evaluating the Use of Phase Change Materials in Concrete Pavement to Melt Ice and Snow. Journal of Materials in Civil Engineering. 2015:04015161.
[27] Sakulich AR, Bentz D. Incorporation of phase change materials in cementitious systems via fine lightweight aggregate. Construction and Building Materials. 2012;35:483-90.
[28] Cabeza LF, Castellon C, Nogues M, Medrano M, Leppers R, Zubillaga O. Use of microencapsulated PCM in concrete walls for energy savings. Energy and Buildings. 2007;39(2):113-9.
[29] Hunger M, Entrop A, Mandilaras I, Brouwers H, Founti M. The behavior of self-compacting concrete containing micro-encapsulated phase change materials. Cement and Concrete Composites. 2009;31(10):731-43.
[30] Pasupathy A, Velraj R, Seeniraj R. Phase change material-based building architecture for thermal management in residential and commercial establishments. Renewable and Sustainable Energy Reviews. 2008;12(1):39-64.
[31] Thiele AM, Kumar A, Sant G, Pilon L. Effective thermal conductivity of three-component composites containing spherical capsules. International Journal of Heat and Mass Transfer. 2014;73:177-85.
[32] Thiele AM, Wei Z, Falzone G, Young BA, Neithalath N, Sant G, et al. Figure of merit for the thermal performance of cementitious composites containing phase change materials. Cement and Concrete Composites. 2016;65:214-26.
[33] Bolander J, Saito S. Fracture analyses using spring networks with random geometry. Engineering Fracture Mechanics. 1998;61(5):569-91.
[34] Schlangen E, Van Mier J. Simple lattice model for numerical simulation of fracture of concrete materials and structures. Materials and Structures. 1992;25(9):534-42.

[35] Grassl P, Jirásek M. Meso-scale approach to modelling the fracture process zone of concrete subjected to uniaxial tension. International Journal of Solids and Structures. 2010;47(7):957-68.
[36] Sands CM. An irregular lattice model to simulate crack paths in bonded granular assemblies. Computers & Structures. 2016;162:91-101.
[37] Šavija B, Liu D, Smith G, Hallam KR, Schlangen E, Flewitt PE. Experimentally informed multi-scale modelling of mechanical properties of quasi-brittle nuclear graphite. Engineering Fracture Mechanics. 2016;153:360-77.
[38] Liu L, Ye G, Schlangen E, Chen H, Qian Z, Sun W, et al. Modeling of the internal damage of saturated cement paste due to ice crystallization pressure during freezing. Cement and Concrete Composites. 2011;33(5):562-71.
[39] Schlangen E, Qian Z. 3D modeling of fracture in cement-based materials. Journal of Multiscale Modelling. 2009;1(02):245-61.
[40] Yip M, Mohle J, Bolander J. Automated modeling of three-dimensional structural components using irregular lattices. Computer-Aided Civil and Infrastructure Engineering. 2005;20(6):393-407.
[41] Bolander JE, Berton S. Simulation of shrinkage induced cracking in cement composite overlays. Cement and Concrete Composites. 2004;26(7):861-71.
[42] Luković M, Šavija B, Schlangen E, Ye G, van Breugel K. A 3D Lattice Modelling Study of Drying Shrinkage Damage in Concrete Repair Systems. Materials. 2016;9(7):575.
[43] Šavija B, Pacheco J, Schlangen E. Lattice modeling of chloride diffusion in sound and cracked concrete. Cement and Concrete Composites. 2013;42:30-40.
[44] Wang L, Ueda T. Mesoscale modelling of the chloride diffusion in cracks and cracked concrete. Journal of Advanced Concrete Technology. 2011;9(3):241-9.
[45] Šavija B, Luković M, Schlangen E. Lattice modeling of rapid chloride migration in concrete. Cement and Concrete Research. 2014;61:49-63.
[46] Pacheco J, Šavija B, Schlangen E, Polder RB. Assessment of cracks in reinforced concrete by means of electrical resistance and image analysis. Construction and Building Materials. 2014;65:417-26.
[47] Lewis R, Nithiarasu P, Seetharamu K. Fundamentals of the Finite Element Method for Heat and Fluid Flow, 2004. John Wiley & Sons; 2004.
[48] Nakamura H, Srisoros W, Yashiro R, Kunieda M. Time-dependent structural analysis considering mass transfer to evaluate deterioration process of RC structures. Journal of Advanced Concrete Technology. 2006;4(1):147-58.
[49] Thiele AM, Sant G, Pilon L. Diurnal thermal analysis of microencapsulated PCM-concrete composite walls. Energy Conversion and Management. 2015;93:215-27.
[50] De Schutter G, Taerwe L. General hydration model for Portland cement and blast furnace slag cement. Cement and Concrete Research. 1995;25(3):593-604.
[51] Van Breugel K. Numerical simulation of hydration and microstructural development in hardening cement-based materials:(II) applications. Cement and Concrete Research. 1995;25(3):522-30.
[52] Ye G. Experimental study and numerical simulation of the development of the microstructure and permeability of cementitious materials: TU Delft, Delft University of Technology; 2003.
[53] Liwu M, Min D. Thermal behavior of cement matrix with high-volume mineral admixtures at early hydration age. Cement and Concrete Research. 2006;36(10):1992-8.
[54] Van Beek A, Baetens B, Schlangen E. Numerical model for prediction of cracks in concrete structures. PRO 23: International RILEM Conference on Early Age Cracking in Cementitious Systems-EAC'01: RILEM Publications; 2002. p. 39.
[55] Schlangen E. Online help/manual module HEAT of FEMMASSE. The Netherlands. 2000.
[56] Zienkiewicz OC, Taylor RL, Taylor RL. The finite element method: McGraw-hill London; 1977.
[57] Aguayo M, Das S, Maroli A, Kabay N, Mertens JC, Rajan SD, et al. The influence of microencapsulated phase change material (PCM) characteristics on the microstructure and strength of cementitious composites: Experiments and finite element simulations. Cement and Concrete Composites. 2016;73:29-41.

[58] Cunha S, Aguiar J, Ferreira V, Tadeu A. Mortars based in different binders with incorporation of phase-change materials: Physical and mechanical properties. European Journal of Environmental and Civil Engineering. 2015;19(10):1216-33.
[59] Neville AM. Properties of concrete: John Wiley & Sons; 1995.